Initial Plasma Confinement Experiments in Tokamak-Helical Hybrid Device TOKASTAR-2

Kazuhisa BABA, Kozo YAMAZAKI, Hideki ARIMOTO, Tetsutarou OISHI, Koki OKANO, Makoto HASEGAWA and Tatsuo SHOJI

Department of Energy Engineering and Science, Graduate School of Engineering, Nagoya University, Furo-cho, Chikusa-ku, Nagoya 464-8603, Japan

(Received 9 December 2009 / Accepted 20 April 2010)

A tokamak-helical hybrid device TOKASTAR-2 with outboard helical field coils located outside the toroidal field coil system was constructed. Initial plasmas are produced by the electron cyclotron heating scheme, and the plasma electron density profile is measured using electrostatic double Langmuir probes. The peak location of measured electron density profile in the radial direction agrees with the first electron cyclotron resonance layer at initial beak-down period and at final disappearance period of the plasma discharge. The suppression of bursting electron density oscillations and the shift of plasma density profile are observed in the case of applying outboard helical magnetic field.

Keywords: tokastar-2, tokamak, helical system, hybrid configuration, Langmuir probe, electron cyclotron heating, electron density profile

DOI: 10.1585/pfr.5.S2036

1. Introduction

Tokamak and helical systems have been widely recognized as efficient toroidal magnetic plasma confinement devices. The machine TOKASTAR-2 is a new plasma confinement device which has both tokamak and helical confinement properties [1, 2]. There are outboard helical field (HF) coils with the toroidal period $N = 2$ or 1 outside eight toroidal field (TF) coils. One of main ultimate purposes of this experiment is to evaluate the effect of external outboard helical field application on tokamak plasma confinement. As an initial confinement experiment, we produced plasmas in simple toroidal field configuration and applied outboard helical field to these plasmas which are created by the electron cyclotron heating (ECH) using 2.45 GHz microwave with pulsed power up to 2 kW. The toroidal plasma current is not inductively induced in this experiment.

In section 2, toroidal magnetic field profile and electron cyclotron resonance (ECR) layer position are calculated in this device, and the spatial profile of plasma electron density measured by double Langmuir probes is compared with this calculation. In section 3 the shift of density profile in ECH plasma is shown when helical magnetic field is applied to a simple toroidal magnetic field configuration. The summary is given in section 4.

2. Toroidal Magnetic Field Profile and Location of ECH Resonance Layer

Magnetic field profile produced by toroidal field (TF)

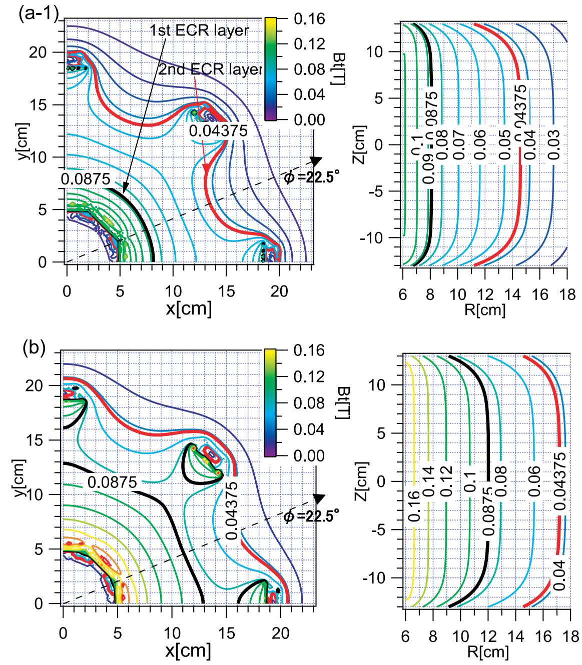

Fig. 1 Contour map of toroidal magnetic field strength. x-y plane at $Z = 4.5$ cm, and R-Z plane at $\phi = 22.5°$, in the case of (a) $I_{TF} = 88.8$ A and (b) $I_{TF} = 135$ A.

coils is calculated using the Biot-Savart's law. The 50-turn toroidal coil filament system is adopted in the calculation to simulate a real 50-turn TF coil block. Figure 1 shows a contour map of toroidal magnetic field strength on x-y plane at $Z = 4.5$ cm and on R-Z plane (poloidal cross-section) at toroidal angle of 22.5 degree. Figure 1 (a)

author's e-mail: baba-kazuhisa09@ees.nagoya-u.ac.jp

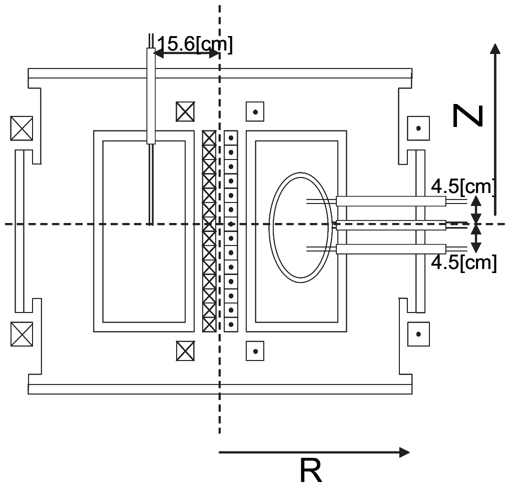

Fig. 2 Arrangement view of three Langmuir probes installed in the TOKASTAR-2.

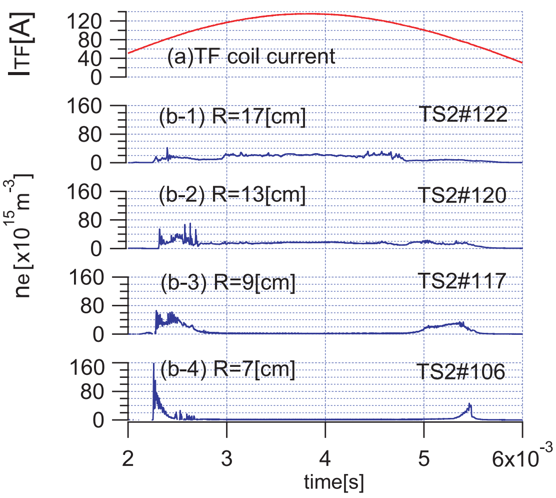

Fig. 3 Time variations of (a) toroidal coil current and (b) four electron density traces at respective measuring points.

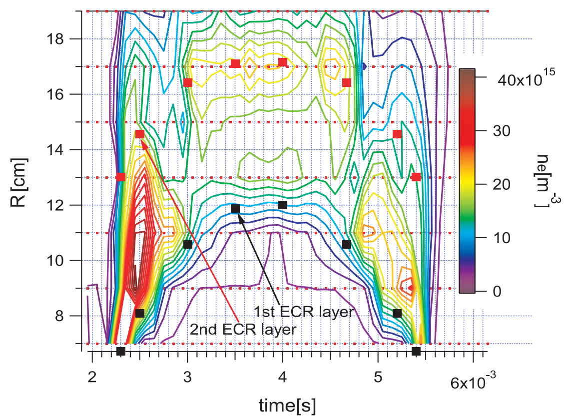

Fig. 4 Contour map of electron density profile in the *R*-direction. Black and red points denote first and second ECR layer location, respectively.

corresponds to TF coil current I_{TF} = 88.8 A, and Fig. 1 (b) to I_{TF} = 135 A. The ECH first resonance layer (0.0875 T) for 2.45 GHz microwave is given by black line in Fig. 1. The ECH second resonance layer is also given by red line. These electron cyclotron resonance (ECR) layers are shown by almost vertical straight line on the poloidal cross section. When the TF coil current increases in time, the ECR layer shifts outward in the radial direction.

Measurement of ion-saturation currents of electrostatic double probe was done to evaluate radial profile of ECH plasma density. The probe tip of 1.5 mm in diameter and 4 mm in length is used. Two ceramic cylinders of 3 mm in outer diameter and ~ 8 cm in length are connected to a 15 mm diameter stainless steel pipe. The interval distance between two probe tips is 6 mm, and the applied voltage between two tips is ~50 V to measure ion saturation currents.

Horizontal probe at Z = 4.5 cm was used for the measurement as shown in Fig. 2. The probe was swept at 2 cm intervals from R = 7 cm to 19 cm. The applied probe voltage is V_d = 46 V for measuring ion-saturation current. Time evolutions of electron density at respective measuring points are shown in Fig. 3. Figures (b-1), (b-2), (b-3) and (b-4) of Fig. 3 correspond to R = 17 cm, 13 cm, 9 cm, 7 cm respectively. These electron density traces are obtained from probe ion-saturation currents I_{is} assuming that the electron temperature T_e is constant at respective measuring points and using Eq. (1),

$$I_{is} = 0.61 e S n_e (kT_e/M)^{1/2}, \qquad (1)$$

where S is probe area, M is ion mass, and I_{is} is ion-saturation current.

The central temperature of plasma is estimated to be about 10 eV from the current-voltage probe property. The density contour map of Fig. 4 was created by shot-by-shot probe current measurements at respective radial direction. Black points and red points indicate ECH first (875 G) and second (438 G) resonance layer, respectively. The peak location of measured plasma density profile agrees with this first ECR layer at the initial break-down period (t = 2.3 ms) and the final disappearance period (t = 5.4 ms) of the plasma discharge. Among middle period (t = 3.0~4.5 ms), it is considered that plasma density profile is determined by second resonant heating effect in this case, where the plasma is produced outside the TF coils. Different from this case, other resonant heating mechanisms such as upper hybrid resonance should be considered in other lower field cases shown later (typically in Fig. 7).

3. Effect of Steady-state Outer Helical Magnetic Field on ECH Plasma

ECH plasmas confined by simple toroidal magnetic field without and with outboard helical magnetic field were compared. Measurement of plasma density profile is done by one vertical probe and two horizontal probes. Vertical probe positions are R = 15.6 cm and two horizontal probe

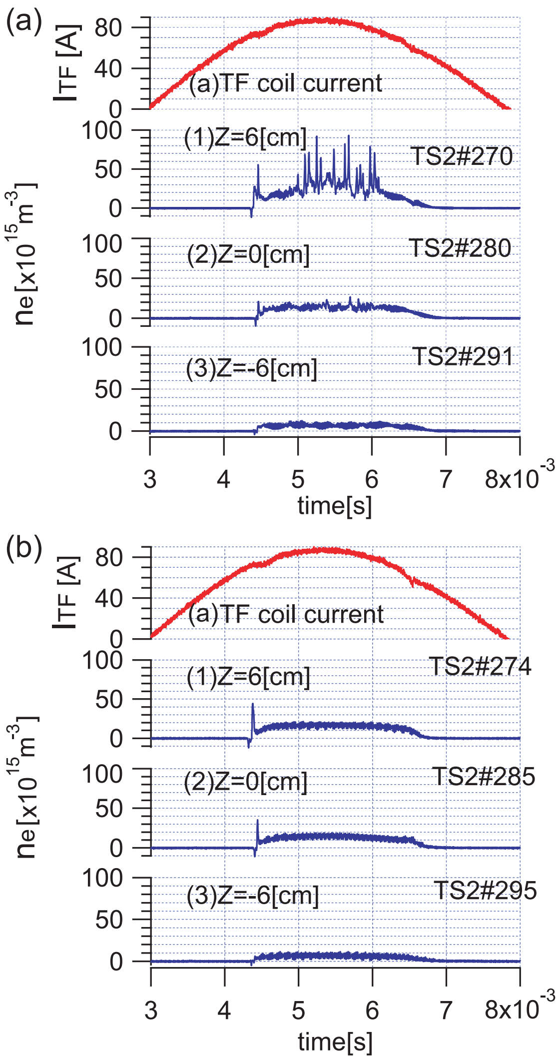

Fig. 5 Toroidal coil current and electron density traces at respective measuring points using vertical probe (a) without and (b) with static helical field application.

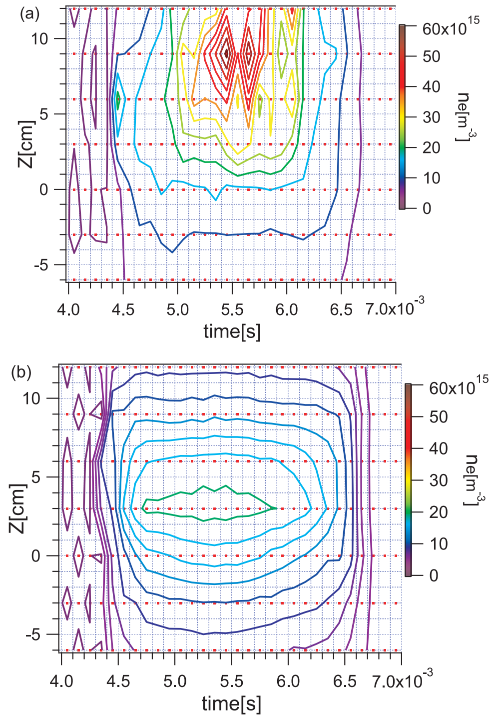

Fig. 6 Contour map of probe current profile in the Z-direction (a) without and (b) with static helical field application.

position is Z = 4.5 cm, -4.5 cm respectively as shown in Fig. 2. The applied voltages of all probes were set to V_d = 56 V for measuring ion-saturation current.

Figure 5 shows time evolution of electron density without and with helical magnetic field application at respective probe measuring point by vertical probe. Bursting oscillations are observed at upper side of the equatorial plane without helical field. But these bursting oscillations are suppressed with static helical field application.

Figure 6 shows a vertical contour map of electron density profile (a) without and (b) with static helical magnetic field application. The upward shift of vertical density profile is reduced when static external helical field is applied, as shown in Fig. 6. The peak absolute value of the probe current, therefore electron density, becomes smaller, and there is a possibility that plasma column will move horizontally in addition to downward vertical shift.

Figure 7 shows a horizontal contour map of plasma density profile in the radial direction at $Z = -4.5$ cm mea-

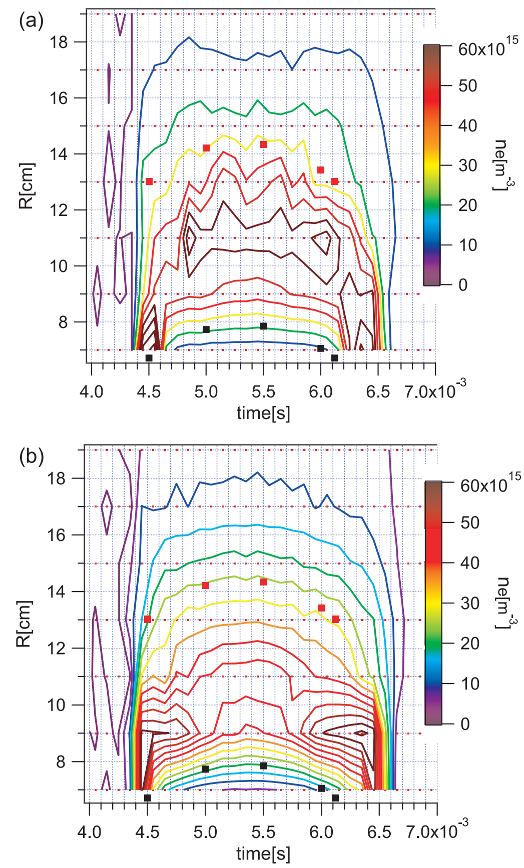

Fig. 7 Contour map of electron density profile ($Z = -4.5$ cm) in the R-direction (a) without and (b) with static helical field application.

sured at the same time of the vertical probe (a) without and (b) with helical magnetic field application. Different from Fig. 2, the peak position of electron density at the middle time period of the plasma discharge exists between first and second ECR layers. The upper hybrid resonance or outward plasma toroidal shift might be related to plasma heating mechanism in this case.

The outward expansion of plasma density profile in the *R*-direction at the middle time period ($t = 5.0 \sim 6.0$ ms) of the plasma discharge can be reduced when an external helical magnetic field is applied, as suggested in Fig. 7. Bursting repetitive toroidal drifts induced by the electric charge separation in a simple toroidal filed configuration might be suppressed by the outboard helical field application.

4. Summary and Discussions

Initial plasma experiments in TOKASTAR-2 were carried out in a simple toroidal filed configuration. The outboard helical field was applied to ECH plasmas.

The peak location of electron density profile in the *R*-direction agrees with first electron cyclotron resonance layer position at initial break-down period and at final disappearance period, but not at the middle time zone of the plasma discharge. Second higher harmonic resonance, upper hybrid resonance, and the effect of toroidal drift are being examined for this density profile.

The bursting oscillations observed at the upper side of the equatorial plane by *Z*-probe are suppressed by applying an external helical magnetic field. The profile shift under *Z*-direction was reduced in the case of helical field application according to the *Z*-probe measurement. The outward plasma expansion in the *R*-direction may be suppressed by the helical field application. Effects of the helical magnetic field application on plasma fluctuation and movement are being examined in details.

[1] K. Yamazaki and Y. Abe, "Tokastar: Tokamak-Stellarator Hybrid with Possible Bean-Shaped Operation", Research Report of the Institute of Plasma Physics, Nagoya, Japan, IPPJ-**718** (1985).

[2] K. Yamazaki, Y. Taira, T. Oishi, H. Arimoto and T. Shoji, J. Plasma Fusion Res. SERIES **8**, 1044 (2009).